The crystallization behavior of GaSb alloy studied by combined in situ x-ray scattering and electrical measurements

Magali Putero[1*], Toufik Ouled-Khachroum[1], Marie-Vanessa Coulet[1], Christophe Muller[1], Carsten Baehtz[2] and Simone Raoux[3]

[1]Aix-Marseille Université, CNRS, IM2NP UMR 7334, 13397 Marseille, France
[2]ESRF, European Synchrotron Radiation Facility, BP 220, Grenoble Cedex, 38043, France.
[3]IBM/Macronix PCRAM Joint Project, IBM T. J. Watson Research Center, P.O. Box 218, Yorktown Heights, New York 10598, USA
*email : magali.putero@im2np.fr

ABSTRACT

The crystallization behavior of stoichiometric GaSb alloy was studied by combined *in situ* synchrotron techniques. It is found that the GaSb film has an unusual behavior with increasing thickness and decreasing density upon crystallization, whereas its electrical behavior remains typical compared to other phase change materials. Furthermore, for the slow heating rate used in this study, a segregation of Sb, revealed by the crystallization of the Sb phase is proposed.

Key words: phase change material, GaSb, phase transition, density, thickness, combined synchrotron measurements.

1. IINTRODUCTION

Phase change random access memories (PCRAM) are one of the more promising candidates to sustain the industrial demand for high density/speed products. The use of phase change materials for non-volatile data storage is due to their physical properties exhibiting a reversible switch between two electrical/optical states [1] linked to a phase transition that occurs on nanosecond timescale and that is thermally induced [2]. Among the suitable phase change materials, Te-based chalcogenide films, are considered to be leading alloys for application in PCRAM [3,4]. However, they may suffer from phase segregation and insufficient data retention [5]. More recently, Te-free and Sb-rich alloys have been proposed, including SnSb [6], GeSb [7] and GaSb [8] alloys. Ga-Sb alloys were demonstrated to show high thermal stability and very fast crystallization [5]. Moreover, the stoichiometric GaSb compound has been shown to have a unusual negative optical contrast whereas its electrical contrast follows the typical behavior for phase change materials with a high resistivity in the amorphous state and a lower one in the crystalline phase [9].

This work focuses on the correlation between the structural and electrical properties upon crystallization in the stoichiometric GaSb alloy by using combined and simultaneous in situ X-ray diffraction (XRD), X-ray reflectivity (XRR) and sheet resistance (Rs).

2. EXPERIMENTS

Thin films of GaSb were deposited on 500nm thick SiO_2 layer on top of Si (001) substrates by DC-sputtering from nominally stoichiometric GaSb target in an argon atmosphere. Simultaneous *in situ* XRD, XRR and sheet resistance (Rs) measurements were performed on the BM20B-Rosendorf beamline at ESRF (Grenoble, France) using an incident photon energy of 11.7 keV and a dedicated vacuum chamber (10^{-6} mbar) equipped with a heating stage and with an aligned 4-point probes sheet resistance set-up [10,11]. XRD, XRR and Rs measurements were simultaneously performed during the layer annealing with a constant heating rate of 2°C/min, from room temperature up to 400°C. XRD pattern were recorded at grazing incidence (θ =1°) using a 1D Mythen detector. A Fast Fourier Transform (FFT) algorithm was used to analyze XRR data: as detailed in previous studies [12], this calculation enables direct extraction of the layer thickness variations from a series of reflectivity patterns. Some XRR curves were also fitted using the classical matrix thin film method analysis in order to extract film thickness and density. The film compositions were determined by Rutherford Backscattering Spectrometry (RBS) before and after annealing.

3. RESULTS AND DISCUSSION

The RBS measurements performed before and after annealing do not show any composition variation. The results indicate that the nominally stoichiometric sputter target produces slightly antimony-rich films Ga/Sb(45:55) with a uncertainty of 0.5 at.%.

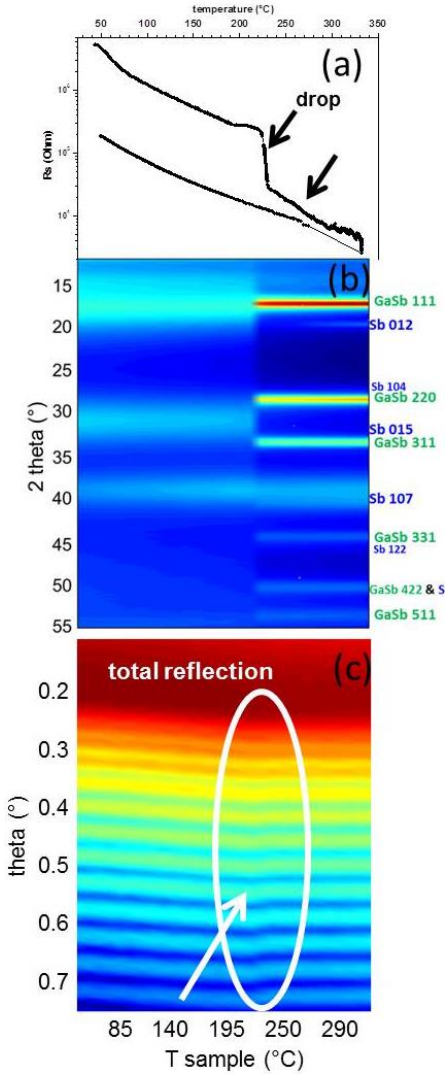

Figure 1: combined in situ Rs (a), XRD (b) and XRR (c) performed simultaneously during thermal annealing.

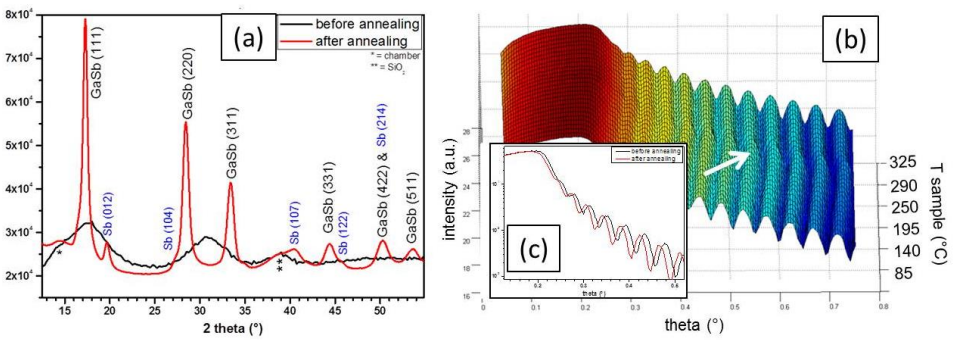

Figure 2: (a) grazing incidence XRD pattern recorded before and after annealing (b) 3D view of the in situ XRR patterns, (c) zoom on the XRR patterns recorded before and after annealing

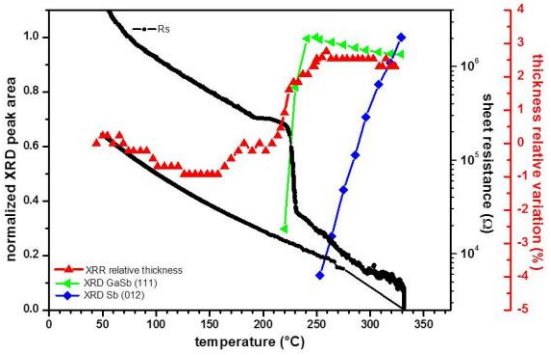

Figure 3: Temperature-dependent evolution of structural and electrical parameters upon annealing extracted from simultaneously performed XRR, XRD and Rs experiments.

Experiment	Crystallization temperature		Density change	Thickness change	Electrical contrast
	GaSb	Sb			
X-ray diffraction	220°C 224°C for I=0.5	253°C 281°C for I=0.5	--	--	--
X-ray reflectivity	221°C		-5.2 ± 0.4	+1.7 ± 0.2 %	--
Sheet resistance	drop 226°C	bump 258°C	--		2.0×10^{1}

Table 1: Summary of the calculated physical parameters. T_B corresponds to the temperature at which the first Bragg reflections are detected, T_X to the temperature at which the normalized integrated intensity is equal to 0.5.

Figs. 1a, 1b and 1c show respectively the results of Rs, XRD and XRR measurements performed simultaneously during the annealing of a GaSb layer. At room temperature, the broad modulations on XRD pattern were indicative of an amorphous phase (Fig. 1b and Fig.2a). At 220°C the onset of several Bragg reflections indicates that crystallization occurs. The pattern indexation shows that these peaks correspond to the cubic structure of GaSb. Interestingly, around 253°C, new Bragg peaks characteristic of the pure rhombohedral Sb phase appear. This shows that an elemental segregation occurs with a separate crystallization of Sb. In order to confirm this result, accurate XRD pattern were recorded after annealing. As seen in Fig. 2a, (012), (107), and (122) Bragg reflections can be indexed without ambiguity. Note that the intensity of the Sb peaks is low as compared to the GaSb ones suggesting that this segregation may concern only a few percent of Sb. Such a phase separation has been already observed in Sb-rich phase change materials such as $Ge_{15}Sb_{85}$ [13,14], but to our knowledge this segregation is reported for the first time in stoichiometric GaSb system. Interestingly, in previous study [9] on similar composition (Ga/Sb(46:54)), the Sb crystallization was not detected. This could be explained by a much slower temperature ramp (2°C/min to be compared to 1°C/s), a larger 2θ range that enables measuring Sb (012) Bragg reflection, and/or a better experimental resolution due to the larger sample-detector distance.

Concomitantly with the crystallization of the GaSb phase, the Rs drastically falls around 226°C (Fig. 1a). This steep drop of Rs can be attributed to a change in the electrical properties of the layer: the decrease of one order of magnitude clearly indicates that GaSb film switches from a high-resistance state to a low-resistance state. Around 258°C, another effect is observed in the Rs curve as evidenced by the arrow in Fig 1.a. This effect may be linked to the crystallization of Sb.

Figure 1c presents a series of XRR patterns (2D view) acquired simultaneously with XRD and Rs measurements. The whole XRR patterns are also shown in 3D view on Fig. 2b. Below 221°C the continuous shift of both the Kiessig fringes and the total reflection edge indicates a small continuous thickness reduction and density increase. Around 221°C, a clear change is observed in the XRR patterns (as indicated by white arrow in Fig. 1c). The total reflection edges at 25°C and after the annealing are also compared in Fig. 2c. The shift of the critical angle for total reflection towards smaller angles indicates a density decrease. This latter decrease in density leads to a volume expansion, which corresponds to an increase in the film thickness actually shown from the shift of Kiessig oscillations towards smaller angles. Above 221°C, XRR patterns do not exhibit drastic changes, even around the Sb crystallization temperature. Using FFT analysis, the layer thickness was estimated to increase from 61.1 nm in the amorphous state to 62.5 nm in the crystalline state at 330°C. Satisfactory XRR curve fitting was also achieved in considering a density decrease of -5.2% ± 0.4% and a thickness increase of +1.7% ± 0.2% before and after annealing. Such a behavior (increasing thickness and decreasing density) upon crystallization is contrasting with observations done in other phase change materials as $Ge_2Sb_2Te_5$ and GeTe alloys [10,15]. It may be linked to the negative optical contrast measured by static laser testing for the stoichiometric GaSb alloy which is also very unusual for phase change materials [9].

To correlate the three *in situ* measurements, the position of XRR FFT peak (i.e. film thickness) and the integrated intensity of the GaSb (111) and Sb (012) Bragg reflections were extracted as a function of temperature. Figure 3 compares on the same plot the evolution of electrical (Rs) and microstructural parameters. For Rs and XRR experiments, the crystallization temperature was determined from the peak in the first derivative as function of temperature. The electrical contrast is also reported in this table. It was derived from the ratio between the Rs at room temperature before annealing (Rs_{before}) and the one after annealing (Rs_{after}). For XRD data, the crystallization temperature was extracted using i) the temperature (T_B) at which the first Bragg reflection appear, and ii) the temperature (T_X) at which the normalized integrated intensity corresponds to 0.5.

As shown in Figure 3 and Table 1, the crystallization temperature deduced from Rs corresponds to the temperature T_B at which the first Bragg reflections are detected. This temperature also matches with the crystallization temperature deduced from XRR. Those three crystallization temperatures being very close, an average value of 222°C ± 4°C can be determined. In early findings on similar samples the crystallization temperature was determined to be 203°C and 223°C using respectively resistivity measurements in van der Pauw geometry and time resolved XRD, but much faster annealing ramp (resp. $5°C.s^{-1}$ and $1°C.s^{-1}$) [9]. Taking the different heating rate into account the values agree well. The same study [9] also reported a maximal electrical contrast of 10^3 on this alloy, that is higher than the value deduced from the Rs measurement shown in Fig.1a and reported in Table 1. However, this discrepancy could be due to the dependence of the resistivity of the crystalline material according to the maximum annealing temperature [9].

4. CONCLUSION

Combined, simultaneous and *in situ* XRR, XRD and Rs measurements were deployed to study the behavior of stoichiometric GaSb alloy upon crystallization. Correlated changes in both structural and electrical properties were evidenced, the GaSb film density, thickness and sheet resistance changing upon crystallization. The GaSb film was found to have an unusual behavior with increasing thickness and decreasing density upon crystallization, which may be linked to its negative optical contrast. However, the electrical behavior remains typical compared to other phase change materials, with a steep drop from high to low resistivity upon crystallization. Furthermore, for the slow heating rate used in this study, a segregation of Sb, revealed by the crystallization of the Sb phase at 253°C, is proposed.

REFERENCES

1. M. Wuttig, N. Yamada, Nature Materials **6** (2007) 824–32.
2. G. Bruns, P. Merkelbach, et al., Applied Physics Letters **95** (2009) 043108.
3. V. Sousa, Microelectronic Engineering **88** (2011) 807–813.
4. S. Raoux, W. Wełnic, D. Ielmini, Chemical Reviews **110** (2010) 240–67.
5. H.-Y. Cheng, S. Raoux, J.L. Jordan-Sweet, Applied Physics Letters **98** (2011) 121911.
6. F. Rao, Z. Song, K. Ren, X. Li, L. Wu, W. Xi, B. Liu, Applied Physics Letters **95** (2009) 032105.
7. S. Raoux, C. Cabral, et al., Journal of Applied Physics **105** (2009) 064918.
8. Y. Lu, S. Song, Z. Song, B. Liu, Journal of Applied Physics 109 (2011) 064503.
9. S. Raoux, A.K. König, et al., Physica Status Solidi (B) **249** (2012) 1999–2004.
10. M. Putero, T. Ouled-Khachroum, et al., Journal of Applied Crystallography **44** (2011) 858–864.
11. M. Putero, B. Duployer, et al., Thin Solid Films (2012) in press, http://dx.doi.org/10.1016/j.tsf.2012.11.131.
12. M. Putero, L. Ehouarne, E. Ziegler, D. Mangelinck, Scripta Materialia **63** (2010) 24–27.
13. L. Krusin-Elbaum, D. Shakhvorostov, C. Cabral, S. Raoux, J.L. Jordan-Sweet, Applied Physics Letters **96** (2010) 121906.
14. P. Zalden, G. Aquilanti, et al., J. of Non-Cryst. Sol. (2013) in press http://dx.doi.org/10.1016/j.jnoncrysol.2013.01.005 .
15. W.K. Njoroge, H.-W. Wöltgens, M. Wuttig, J. of Vac. Sc. & Tech.y A: 20 (2002) 230.